Cosmological Flashes from Rotating Black Holes

Maurice H.P.M. van Putten

LIGO Laboratory, MIT 17-161, 175 Albany Street, Cambridge, MA 02139

ABSTRACT

Current phenomenology suggests the presence of a compact baryon-poor energy source to cosmological gamma-ray bursts reacting to high-density matter. The association of short and long gamma-ray bursts with hyper- and suspended accretion onto slowly and rapidly spinning black holes predicts weak X-ray afterglow emissions from short bursts, as in GRB050509B and GRB050709. Long gamma-ray bursts are probably the birth place of rapidly spinning high-mass black holes in core-collapse of massive stars, as in GRB030329 with supernova SN2003dh. This predicts a long-duration burst of gravitational radiation powered by the spin-energy of the black hole. In contrast to MeV-neutrino emissions, as in SN1987A, this can be tested by the advanced detectors LIGO and Virgo about once per year up to distances of about 100Mpc. Detection of the expected chirps and long-duration bursts of gravitational waves promises identification of Kerr black holes as the most luminous objects in the Universe.

Subject headings: gamma rays:bursts — gravitational waves

1. Introduction

Gammma-ray bursts (GRBs) were discovered serendipitously as "flashes in the sky" by the nuclear test-ban monitoring satellites Vela (US) and Konus (USSR). These were soon recognized to be a natural phenomenon. The first data were publicly released by Klebesadel et al. (1973) and Mazets et al. (1974). The mysterious origin of this new astrophysical transient, lasting up to tens of seconds in non-thermal gamma-ray radiation, gradually triggered a huge interest from the high-energy astrophysics community. The Burst and Transient Source Experiment (BATSE) on NASA's Compton Gamma-Ray Observatory, launched in 1991, identified an isotropic distribution in the sky and revealed the existence of short and long gamma-ray bursts, whose durations are broadly distributed around 0.3s and 30s, respectively (Kouveliotou et al. 1993; Paciesas 1999). Moreover, the sensitivity of BATSE showed a deficit in faint bursts in the number-versus-intensity distribution distinct from a -3/2 powerlaw. Meegan et al. (1992) hereby established that gamma-ray bursts are of cosmological

origin. More recently, the Italian-Dutch satellite BeppoSax discovered X-ray flashes (Heise et al. 2000), which may be closely related to long gamma-ray bursts. Their non-thermal emissions are herein best accounted for by internal shocks in ultrarelativistic outflows in the fireball model proposed by Rees & Mészáros (1992, 1994) – with unknown inner engine producing these baryon-poor outflows. If gravitationally powered, their compact size, based on short-time scale variabilities in the gamma-ray lightcurves, may involve the formation of black holes surrounded by a high-mass torus (Paczyński 1991; Woosley 1993).

At cosmological distances, the isotropic equivalent luminosities are on the order of 10^{51} erg s^{-1} – as bright as 10^{18} solar luminosities. These events, widely acclaimed as the "Biggest Bang since the Big Bang", are now known to light up the Universe about once per minute. What, then, is their origin? The most powerful observational method to encyst the enigmatic energy source is through *calorimetry on all radiation channels*. This involves measuring the energy output in emissions in the electromagnetic spectrum, as well as in yet "unseen" emissions in neutrinos and gravitational waves. Perhaps thus shall we be in a position to determine their constitution, and decide whether their inner engine is *baryonic*, such as a neutron star, or *non-baryonic*: a black hole energized by spin. The exact solution of Roy P. Kerr (1963) – see Table I for a parametrization – shows an energy per unit mass which is anomalously large at high spin rates, exceeding that of a rapidly spinning neutron by an order of magnitude. By this potentially large and baryon-free energy reservoir, a Kerr black hole is a leading candidate for the inner engine of GRBs, at least those of long-durations in view of the following observational results.

The Italian-Dutch BeppoSax satellite, launched in 1996, dramatically changed the landscape of long GRBs with the discovery by E. Costa (Costa et al. 1997) of X-ray afterglows in GRB970228 (confirmed in observations by the ASCA and ROSAT satellites). These lower-energy emissions permit accurate localizations, enabling follow-up by optical telescopes. Thus, J. van Paradijs (van Paradijs et al. 1997) pointed the Isaac Newton Telescope and the William Herschel Telescope to further discover optical emissions associated with the same event. These lower-energy X-ray and optical emissions agree remarkably well with the expected decay of shocks in ultrarelativistic, baryon-poor outflows in the previously developed fireball model. Even lower-energy, radio-afterglows have been observed in some cases, including GRB970228 (Frail et al. 1997). The same optical observations have now led to tens of GRBs with individually measured redshifts, up to $z = 6.29$ in GRB050904 detected by the recently launched Swift satellite (Chincarini et al. 2005; Haislip et al. 2005).

Optical follow-up identified the association of long GRBs with supernovae. In particular, the unambiguous association of GRB030329 with SN2003dh ($z = 0.167$, $D = 800$Mpc) (Stanek et al. 2003) identified Type Ib/c supernovae as the parent population of long GRBs

(Fig. 1). This observation confirms their association with core-collapse supernovae of massive stars, proposed by S. Woosley (Woosley 1993; Katz 1994; Paczyński 1998). Massive stars have characteristically short lifetimes, whereby GRB-supernovae track the cosmological event rate. This conclusion is quantitatively confirmed by consistent estimates of the true-to-observed GRB-SNe event rate of 450-500 deduced from two independent analysis, based on geometrical beaming factors (Frail et al. 2001) and locking to the star-formation rate (van Putten & Regimbau 2003). These event rates correspond to a true cosmological event rate of about one per minute.

Core-collapse supernovae from massive stars are believed to produce neutron stars or black holes. The former are perhaps best known from the rapidly spinning neutron star (a pulsar) in the Crab nebula, a remnant of what was probably a Type II supernova in 1054. The second is more difficult to ascertain with certainty, such as in the more recent Type II event SN1987 in the Large Megellanic Cloud. At close proximity, its burst in MeV-neutrinos was detected by Kamiokanda and IMB (see Burrows & Lattimer (1987)) which provided direct evidence for the formation of matter at nuclear densities. The absence of a pulsar or a point-source of X-ray radiation in this case suggests continued collapse – probably into a stellar mass black hole.

Type II and Type Ib/c supernovae are both believed to represent the endpoint of massive stars (Filipenko 1997; Turatto 2003), and possibly so in binaries such as the Type II/Ib event SN1993J (Maund et al. 2004). This binary association suggests a hierarchy, wherein hydrogen-rich, envelope–retaining SNII are associated with wide binaries, while hydrogen-poor, envelope–stripped SNIb and SNIc are associated with increasingly compact binaries (Nomoto et al. 1995; Turatto 2003). By tidal coupling, the primary star in the latter will rotate at approximately the orbital period at the moment of core–collapse. With an evolved core (Bethe et al. 2003), these Type Ib/c events in particular are believed to produce a spinning black hole (Woosley 1993; Paczyński 1998; Brown et al. 2000; Lee et al. 2002). However, the branching ratio of Type Ib/c into GRB-supernovae is small,

$$\mathcal{R}(\mathrm{SNIb/c} \to \mathrm{GRB}) = \frac{N(\mathrm{GRB\text{-}SNe})}{N(\mathrm{SNIb/c})} \simeq (2-4) \times 10^{-3} \qquad (1)$$

as calculated from the true GRB-supernova event rate relative to the observed event rates of supernovae of Type II and Type Ib/c. This ratio is remarkably small, suggesting a higher-order down-selection process.

The identification of long GRBs with core-collapse supernovae brings into scope their potential gravitational-wave emissions. This may be due to a variety of mechanisms associated with rapidly rotating fluids. In particular, emissions will be produced by bar-mode instabilities producing fragmentation of orbiting matter prior to the formation of a compact

object (Nakamura & Fukugita 1989; Bonnel & Pringle 1995) or in the formation of multiple compact objects (Davies et al. 2002), non-axisymmetries in accretion disks (Papadopoulos & Font 2001; Mineshige et al. 2002; Kobayashi & Mészáros 2003a,b), as well as after the formation into a rapidly spinning black hole. The first may produce an initial "splash" of gravitational radiation (Rees et al. 1974), the second a bi-model spectrum containing high-frequency emissions produced by non-axisymmetric perturbations of the black hole and low-frequency emissions from the disk, whereas the latter creates a long-duration burst of low-frequency gravitational radiation. Calculations this time-evolving spectrum of gravitational-radiation are only beginning to be addressed by computational hydro- and magnetohydrodynamics, during initial collapse (Rampp et al. 1998; Fryer et al. 1999; McFadyen & Woosley 1999; Fryer et al. 2002; Duez et al. 2004) and in the formation of a non-axisymmetric torus (Bromberg et al. 2005). Emissions from matter surrounding a stellar-mass black hole are in the frequency range of sensitivity of the gravitational-wave experiments LIGO (Abramovici et al. 1992; Barish & Weiss 1999) and Virgo (Bradaschia et al. 1992; Acernese et al. 2002; Spallici et al. 2004). Understanding their wave-forms can serve strategic search-and-detection algorithms, triggered by gamma-ray observations (Finn et al. 2004) or by their associated supernova. The latter is more common by the aforementioned true-to-observed event ratio of GRB-supernovae.

In this review, we shall discuss a theory of GRBs from rotating black holes. Current phenomenology on GRB-supernovae poses a challenge to model

- The durations of long GRBs of tens of seconds
- The formation of an associated aspherical supernova
- The launch of ultrarelativistic jets with beamed gamma-ray emissions
- A small branching ratio of Type Ib/c supernovae into GRBs of less than 0.5%

This phenomenology will be directly linked to the spin energy of the black hole. Quite generally, we are left with the task of modeling all possible radiation channels produced by the putative Kerr black hole, including gravitational radiation, MeV-neutrino emissions, and magnetic winds.

Just as lower-energy X-ray and optical afterglow emissions linked long GRBs to supernovae, we expect that the detection of a contemporaneous burst in gravitational-radiation will lift the veil on their enigmatic inner–engine. A precise determination of this link will enable the identification of a Kerr black hole. The same might apply to Type II and Type Ib/c supernovae.

Understanding the energy source of long GRBs might tell us also about the constitution of short GRBs. The first *faint* X-ray afterglows have been detected of the short event GRB050509B by Swift (Gehrels et al. 2005) and GRB050709 by HETE-II (Villasenor et al. 2005; Fox et al. 2005; Hjörth et al. 2005), further providing the low redshifts $z = 0.225$ and $z = 0.16$, respectively. The nature of host galaxies, preferably (older) elliptical galaxies for short bursts versus (young) star-forming galaxies for long bursts, supports the origin of short events in binary coalescence of black holes and neutron stars (Piro 2005). After completion of this review, Kulkarni (2005) outlined a very interesting prospect for long-lasting supernova-like signatures to short bursts from the debris of a neutron star binary coalescence with a similar partner or black hole.

Earlier, we explained the dichotomy of short and long events in terms of hyper- and suspended accreting onto slowly and rapidly rotating black holes, respectively (van Putten & Ostriker 2001). Thus, we predicted similar X-ray afterglows with the property that those to short events are relatively faint: *the short burst is identical to the final moment of a long burst of gamma-rays*. Hyperaccreting, slowly rotating black holes can be produced through various channels. Black-hole neutron star binaries are remnants of core-collapse events in binaries (Bethe et al. (2003); unless formed by capture in dense stellar clusters). Any rapidly spinning black hole will be spun-down in the core-collapse process, possibly representing a prior GRB-supernova event (this review). The merger of a neutron star onto a black hole (Paczyński 1991) could produce a state of hyperaccretion and produce a short gamma-ray burst. This scenario is consistent with the predominance of long over short events. Less clear is the potential for gamma-ray emissions from the merger of two neutron stars (e.g. Zhuge et al. (1994); Faber et al. (2004)) which, however, should also produce a slowly rotating black hole. Finally, slowly rotating black holes can also be produced in core-collapse of massive star in isolation or a wide binary. Here as well, may detection of their gravitational-wave emissions provide a probe to differentiate amongst these different types of short bursts.

In §2, we give a practical outlook on Kerr black holes and gravitational radiation. In §3, we review the formation and evolution (kick-velocities, growth and spin–down) of Kerr black holes in core–collapse supernovae. This includes the process of converting spin–energy into radiation and estimates on the lifetime of rapid spin. In §4, we calculate multipole mass-moments in a torus due to a hydrodynamical instability. By asymptotic analysis, the energies in the various radiation channels are given in §5. An mechanism for launching ultrarelativistic jets from rotating black holes by a small fraction of black hole spin is given in §6. Specific predictions for these "flashes" as sources for the observatories LIGO and Virgo are given in §7.

2. Theoretical background

Kerr black holes and gravitational radiation are two of the most dramatic predictions of general relativity (other than cosmology). While evidence for Kerr black holes, in particular in their role as powerful inner engines, remains elusive, the quadrupole formula for gravitational radiation has been confirmed observationally with great accuracy.

2.1. Energetics of Kerr black holes

The Kerr metric describes an exact solution of a black hole spacetime with nonzero angular momentum. It demonstrates the remarkable property of *frame-dragging*: the angular velocity ω of otherwise zero-angular momentum observers in spacetime outside the black hole. Frame-dragging assumes a maximal and constant angular velocity Ω_H on the event horizon of the black hole, and decays with the cube of the distance to zero at large distances. This introduces an angular velocity Ω_H of the black hole, as well as *differential* frame-dragging by a non-zero gradient (whereby it is not gauge effect). The aforementioned energy reservoir in angular momentum satisfies,

$$E_{rot} = 2M \sin^2(\lambda/4) = M_{irr} \left(\sqrt{1 + (2M\Omega_H)^2} - 1 \right), \tag{2}$$

where $\sin \lambda$ denotes the specific angular momentum of the black hole per unit mass. Here, we use geometric units with Newton's constant $G = 1$ and velocity of light $c = 1$. These properties give Kerr black holes the potential to react energetically to their environment. They hereby have to potential of serving as universal sources of energy, distinct from any known baryonic object and with direct relevance to the phenomenology of GRBs.

Rotating objects have a general tendency to radiate away their energy and angular momentum in an effort to reach a lower energy state. In the dynamics of rotating fluids, this is described by the well-known Rayleigh stability criterion. In many ways, black hole radiation processes are governed by the same principle. The second law of thermodynamics $dS \geq 0$ for the entropy S shows that the specific angular momentum of a Kerr black hole ($\Omega_H \leq 1/2M$) increases with radiation:

$$a_p \equiv \frac{-\delta J_H}{-\delta M} \geq \Omega_H^{-1} \geq 2M > M \geq a \tag{3}$$

for a black hole of mass M and angular momentum J_H which emits a particle with specific angular momentum a_p. Generally, black holes in isolation are stable by exponential suppression of spontaneous emissions by canonical angular momentum barriers (Unruh 1974;

Hawking 1975; Press & Teukolsky 1972; Teukolsky 1973, 1974). Fortunately, magnetic fields can modulate and suppress these angular momentum barriers.

The earliest studies of active black holes focus on energy-extraction processes in the ergosphere, i.e.: scattering of positive energy waves onto rotating black holes – superradiant scattering of Zel'dovich (1971), Press & Teukolsky (1972), Starobinsky (1972) and Bardeen et al. (1972) – as a continuous-wave analogue to the process of Penrose (1969). A steady-state variation can be found in the process of spin–down through horizon Maxwell stresses, proposed Ruffini & Wilson (1975) and extended to force-free magnetospheres by Blandford & Znajek (1977). Quite generally, therefore, magnetic fields are required as a mediating agent to stimulate luminosities which are of astrophysical interest.

Generally, stellar mass black holes produced in core-collapse of a massive star are parametrized by their mass, angular momentum and kick velocity (M, J, K). The equilibrium electric charge of the black hole which arises in its lowest magnetic energy state, is relevant in sustaining adequate horizon magnetic flux especially at high spin–rates, but is insignificant relative to the spin-energy of the black hole.

2.2. Linearized gravitational radiation

Gravitational-wave emissions are predominantly due to low multipole mass-moments. The quadrupole radiation formula according to the linearized theory of general relativity has been given by Peters & Mathews (1963)

$$L_{gw} = \frac{32}{5} \left(\omega \mathcal{M}\right)^{10/3} F(e), \tag{4}$$

where $F(e)$ is a function of the ellipticity e of a binary with orbital frequency ω and chirp mass $\mathcal{M}$.

This linearized result has been observationally confirmed to within 0.1% by decade-long observations of the Hulse-Taylor binary neutron star system PSR1913+16 (with ellipticity $e = 0.62$, Hulse & Taylor (1975); Taylor (1994)). Its gravitational-wave luminosity of about about 0.15% of a solar luminosity $L_\odot = 4 \times 10^{33}$ erg s^{-1} gives a binary lifetime of about 7.4 Gyr. Encouraged by this observational confirmation, we apply (4) to a non-axisymmetric matter surrounding a black hole. With orbital period $\omega \simeq M_H^{1/2}/R^{3/2}$, $\mathcal{M} \simeq M_H(\delta M_T/M_H)^{5/3}$ and ellipticity $e \simeq 0$, this predicts

$$L_{gw} \simeq \frac{32}{5} \left(\frac{M_H}{R}\right)^5 \left(\frac{\delta M_T}{M_H}\right)^2 \tag{5}$$

The quadrupole moment is due to a mass-inhomogeneity δM_T in the torus. A quadrupole moment appears spontaneously due to non-axisymmetric waves, such as a hydrodynamical or magnetohydrodynamical instability. A detailed description of radiation by all multipole mass-moments in a torus is given in Bromberg et al. (2005).

These existing approaches to energy extraction from rotating black holes do not elucidate the "loading problem:" the diversity in radiation channels and their various energy outputs. This defines a novel challenge for Kerr black holes as inner engines to gamma-ray bursts. These events, perhaps including core-collapse supernovae, pose the potential for a powerful link between Kerr black holes and gravitational radiation, as outlined below.

3. Formation and evolution of black holes in core-collapse SNe

While all SNIb/c might be producing black holes, only some are associated with GRB-supernovae in view of the observed small branching ratio (1). Black holes produced in *aspherical* core-collapse receive typical kick velocities of a few hundred km s^{-1} (Bekenstein 1973), measured relative to the center of mass of the progenitor star. Such objects inevitably escape from the central high-density region of the progenitor star, even before core-collapse is completed. A small sample of black holes receive low kick-velocities at birth. Remaining centered, these grow into rapidly spinning high-mass black holes by infall of a substantial fraction of the progenitor He-core mass (Fig. 2). This forms a starting point for the parametrization of rotating black holes as inner engines to GRB-supernovae.

The state of matter surrounding the newly formed black hole in core-collapse supernovae is unique, in attaining temperatures of in excess of 1MeV (Woosley 1993) and masses of up to a few percent of the mass of the black hole (van Putten & Levinson 2003). We further expect these accretion disks to be magnetized, representing a remnant magnetic field of the progenitor star and modified by a dynamo action in the disk.

The angular velocity Ω_H of the black hole easily exceeds that of surrounding matter, even at relatively low spin-energies. When a surrounding disk is largely unmagnetized, the black hole continues to accrete, enlarging it and spinning it up towards an extreme Kerr black hole along a *Bardeen trajectory* (Bardeen 1970), shown in Fig. 2. Alternatively, the surrounding matter can be magnetized and, fairly generally, may contain an appreciable $m = 0$ component of poloidal flux on average or, when time-variable, with non-zero standard deviation. Topologically, this component represents a uniform magnetization, corresponding to two counter-oriented current rings (van Putten & Levinson 2003). Under these conditions, a torus can form in a state of suspended accretion with angular velocity $\Omega_T < \Omega_H$. This

introduces a channel for *catalytic* conversion of spin–energy into various radiation channels (van Putten & Levinson 2003), forcing the black hole to spin down until the angular velocities become similar $\Omega_H \simeq \Omega_T$.

3.1. Catalyzing black–hole spin–energy

A magnetized torus surrounding a black hole is expected to form in both black hole-neutron star coalescence and core–collapse of a massive star with very similar topological properties (Fig. 3). A magnetized star can be represented to leading order by a single current loop or equivalently a density of magnetic dipole moments. Stretching is around the black hole, as in tidal break-up, or by excision of the center of the star, as in core-collapse into a new black hole, leaves a magnetized annulus consisting of two counter-oriented current rings. Thus, core-collapse supernovae and binary black hole-neutron-star coalescence both give the same outcome: a black hole surrounded by a magnetized torus. In practice, the resulting magnetic field will be modified by turbulence and, possibly, a dynamo.

We can look at the structure of the magnetic field of a torus by inspecting its shape in a poloidal cross-section, and by comparison with pulsar magnetospheres. In case of a pulsar, we see magnetic flux-surfaces of closed magnetic field-lines that reach an outer light cylinder, while open magnetic field-lines extend outwards to infinity. The same structure is found with regards to the torus' outer face, when viewed in poloidal cross-section. Since the event horizon of the black hole is a null-surface, it has the same radiative boundary condition as asymptotic infinity (Blandford & Znajek 1977; Thorne et al. 1986; Okamoto 1992), except for its finite surface area (and surface gravity). It follows that the structure of magnetic field-lines found in a magnetized neutron star also applies to the torus' inner face. For the same reason that a spinning neutron star transfers angular momentum to infinity, the inner face of the torus gains angular momentum from the black hole, whenever the latter spins more rapidly. This produces a *spin–connection by topological equivalence to pulsars*.

Angular momentum transport is by Alfvén waves emitted from the surface of the torus, carrying positive angular momentum waves off the outer face to infinity and negative angular momentum off the inner face into the black hole. In this process, the outer face becomes sub-Keplerian and the inner face becomes super-Keplerian. On balance of the competing torques between these two faces (van Putten & Levinson 2003), this produces a state of suspended accretion (van Putten & Levinson 2003). The angular velocity of a Kerr black hole can reach $\Omega_H = 1/2M$, which far surpasses that of an accretion disk or torus. The black-hole

spin–energy (2) can be transferred to a torus with angular velocity Ω_T with efficiency

$$\eta = \frac{\Omega_H}{\Omega_T}. \tag{6}$$

The task is now to quantify the various radiation channels provided by the torus. We shall discuss these in the next sections.

The process of formation and spin–down of a Kerr black hole has been proposed to quantitatively model the supernovae by various groups (Brown et al. 2000; Bethe et al. 2003; van Putten & Levinson 2003). This approach represents a special case of aspherical, magneto-rotationally driven core-collapse supernovae, notably discussed for Type II supernovae by Bisnovatyi-Kogan (1970); LeBlanc & Wilson (1970); Bisnovatyi-Kogan et al. (1976); Kundt (1976); Wheeler et al. (2000); Akiyama et al. (2003).

3.2. Durations and lifetime of rapid spin

A given torus can support a finite poloidal magnetic field-energy. This is due to an instability, produced by magnetic moment-magnetic moment self-interactions in the fluid.

Instability criteria can be derived for both tilt and buckling (van Putten & Levinson 2003). For a tilt instability between two counter-oriented current rings, representing a uniformly magnetized torus, these interactions are described by a potential

$$U_\mu(\theta) = -\mu B \cos\theta, \tag{7}$$

where μ denotes the magnetic moment dipole moment of the inner ring, B denotes the magnetic field produced by the outer ring, and θ denotes the angle between μ and B. Note that $U_\mu(\theta)$ has period 2π, is maximal (minimal) when μ and B are parallel (antiparallel). For the buckling instability, the same interaction energies arise in the azimuthal partition of the torus into small current rings which, combined, are equivalent to the two counter-oriented current rings.

The central potential well of the black hole provides a stabilizing contribution. As the magnetic moment-magnetic moment interactions act primarily to introduce vertical displacements between two current rings (about their equilibrium configuration in the equatorial plane), we can focus on vertical displacements of fluid elements along surfaces of constant cylindrical radius R. This is distinct from motions of a rigid ring, whose fluid elements move on surfaces of constant spherical radius. In particular, the tilt of a current ring hereby changes the distance to the central black hole according to $\rho = \sqrt{R^2 + z^2} \simeq R(1 + z^2/2R^2)$. In the approximation of equal mass in the inner and outer face of the torus, simultaneous tilt

of one ring upwards and the other ring downwards is associated with the potential energy (van Putten & Levinson (2003), corrected)

$$U_g(\theta) \simeq -\frac{M_T M_H}{R}\left(1-\frac{1}{2}\tan^2(\theta/2)\right) \tag{8}$$

with $\tan(\theta/2) = z/R$ upon averaging over all segments of a ring. Note that $U_g(\theta)$ has period π and is minimal at $\theta = 0$. Similar expressions hold for an azimuthal distribution of current rings. Stability is accomplished provided that the total potential energy $U(\theta) = U_\mu(\theta)+U_g(\theta)$ satisfies $U''(\theta) > 0$. We find the following poloidal magnetic field-to-kinetic energy ratios

$$\frac{\mathcal{E}_B}{\mathcal{E}_k} \simeq \begin{cases} \frac{1}{6} & \text{tilt instability} \\ \frac{1}{15} & \text{bucking instability} \end{cases} \tag{9}$$

in the approximation $\mathcal{E}_B = B^2R^3/6$, representing the poloidal magnetic field-energy of the inner torus magnetosphere in a characteristic volume $4\pi R^3/3$ and $\mathcal{E}_k = M_T M_H/2R$. We next discuss the physical parameters at this point of critical stability, which we interpret as a practical limit on the magnetic field energy that the torus can support.

For a pair of rings of radii $R_\pm$, $(R_+ - R_-)/(R_+ - R_-) = O(1)$, we have $U_\mu(\theta) = (1/2)B^2R^3\cos\theta$, so that the point of critical stability, $U''(\theta) = 0$, gives for the critical magnetic field-strength $B_c^2M_H^2 = (1/4)(M_H/R)^4(M_T/M_H)$, or

$$B_c = 10^{16}\mathrm{G}\left(\frac{7M_\odot}{M_H}\right)\left(\frac{6M_H}{R}\right)^2\left(\frac{M_T}{0.03M_H}\right)^{1/2}, \tag{10}$$

with critical poloidal magnetic field-energy (9).

Rotating black holes with $\Omega_H \gg \Omega_T$ dissipate most of their spin–energy "unseen" in the event horizon. The lifetime of rapid spin is thus

$$T_s \simeq \frac{E_{rot}}{T\dot{S}_H}, \quad T\dot{S}_H \simeq \Omega_H^2 A_\phi^2, \tag{11}$$

where $2\pi A_\phi$ denotes the horizon flux, taking into account that most of the black-hole luminosity is incident onto the inner face of the torus. We then have

$$T_s \simeq 45\mathrm{s}M_{H,7}\eta_{0.1}^{-8/3}\mu_{0.03}^{-1}E_{0.5}^{rot}, \tag{12}$$

where the subscripts denote normalization constants, i.e.: $M_{H,7} = M_H/M_\odot$, $\eta_{0.1} = \eta/0.1$, $\mu_{0.03} = M_T/0.03M_H$ and $E_{0.5}^{rot} = E_{rot}/0.5E_{rot,max}$ corresponding to $\sin\lambda = 0.8894$ in (2). This estimate agrees well with the observed durations of tens of seconds of long GRBs shown in Fig. (1) and statistics of the BATSE catalogue (Kouveliotou et al. 1993).

4. Formation of multipole mass-moments

A torus tends to be unstable to a variety of symmetry-breaking instabilities. This provides a spontaneous mechanism for the creation of multipole mass-moments. Provided that the torus is not completely disrupted, such multipole mass-moments ensure that the torus is luminous in gravitational radiation, when its mass reaches a few percent of that of the black hole. These instabilities can take the form of hydrodynamic and magnetohydrodynamic instabilities.

Papaloizou & Pringle (1984) describe a hydrodynamic buckling instability in infinitesimally slender tori, due to a coupling of surface waves on a super-Keplerian inner face and a sub-Keplerian outer face. This theory can be extended to tori of arbitrary slenderness to be of practical interest (below). In a recent numerical study, the magnetic moment-magnetic moment self-interactions of a uniformly magnetized torus are also found to produce instabilities – buckling instabilities in the poloidal plane (Bromberg et al. 2005). This fully nonlinear numerical study, though one-dimensional, recovers our heuristic analytical bound on the maximal poloidal magnetic field energy-to-kinetic energy in the torus (9). It confirms that the dominant emission channel in gravitational radiation is through the quadrupole mass-moment. These are but two example calculations on the more general challenge of computing gravitational-wave spectra of magnetized tori in suspended accretion. Below, we discuss the hydrodynamic buckling instability for wide tori.

The dynamical stability of a torus with sub-Keplerian outer face and super-Keplerian inner face can be studied in the limit of an inviscid incompressible fluid with Newtonian angular velocity (Papaloizou & Pringle 1984; Goldreich et al. 1986)

$$\Omega(r) = \Omega_a \left(\frac{a}{r}\right)^q \quad (3/2 \leq q \leq 2). \tag{13}$$

Here, q denotes the rotation index which is bounded between the Keplerian value $q = 3/2$ and Rayleigh's stability limit $q = 2$.

Irrotational perturbations to the underlying flow (vortical if $q \neq 2$) remain irrotational by Kelvin's theorem. In studying their stability we consider the harmonic velocity potential in cylindrical coordinates (r, θ, z)

$$\phi = \Sigma_n a_n(r, \theta, z) z^n, \quad \Delta\phi = 0. \tag{14}$$

The equations of motion can be expressed in a local Cartesian frame (x, y, z) with Newtonian angular velocity $\Omega_a = M^{1/2} a^{-3/2}$, equal to the angular velocity of the torus at its major radius $r = a$ about a central mass M. These Cartesian coordinates are related to cylindrical coordinates (r, θ) according to $x = r - a$, $\partial_x = \partial_r$ and $\partial_y = r^{-1}\partial_\theta$. Together with zero-enthalpy boundary conditions on the free inner and outer surface of the torus, we obtain

a complete problem for linearized stability analysis. This problem can be solved semi-analytically, by searching numerical for points of change in stability (Keller 1987) of harmonic perturbations $e^{im\theta - i\omega' t}$ of infinitesimal amplitude at frequency ω' as seen in a corotating frame at $r = a$. Fig. 4 shows the numerical stability diagram.

In general, we encounter for each m a critical rotation index $q = q(b/a, m)$ which depends on the minor-to-major radius b/a of the torus. These curves can be found using numerical continuation methods (Keller 1987). The stability diagram for the rotation index is shown in Fig. 4. In particular, we mention the critical values

$$b/a = 0.7506, 0.3260, 0.2037, 0.1473, 0.1152, \cdots, 0.56/m \tag{15}$$

for the various m-modes at the Rayleigh stability line $q = 2$.

5. Radiation-energies by a non-axisymmetric torus

Rotating black holes in suspended accretion dissipate most of their rotational energy (2) "unseen" in their event horizon, while a major fraction (6) is incident into the inner face of the surrounding torus. This lasts for the lifetime of rapid spin (12), whose tens of seconds represents a secular timescale relative to the millisecond period of the orbital motion of the torus. This reduces the problem of calculating the radiation output from the torus to algebraic equations of balance in energy and angular momentum flux, taking into account the channels of gravitational radiation, MeV-neutrino emissions and magnetic winds. The equations of suspended accretion are

$$\begin{aligned} \tau_+ &= \tau_- + \tau_{gw} \\ \Omega_+ \tau_+ &= \Omega_- \tau_- + \Omega_T \tau_{gw} + P_\nu, \end{aligned} \tag{16}$$

where $(\tau_\pm, \Omega_\pm, \Omega_T = (\Omega_+ + \Omega_-)/2)$ denote the torques on and angular velocities of the inner and outer face of the torus due to surface Maxwell stresses as those on a pulsar, τ_{gw} denotes the torque on the torus due to the emission of gravitational radiation with luminosity $L_{gw} = \Omega_T \tau_{gw}$ and P_ν the power in MeV-neutrino emissions due to dissipation. (The results show temperatures of a few MeV.) These equations are closed by a constitutive relation for the dissipation process. We set out by attributing dissipative heating to magnetohydrodynamical stresses. This introduces an overall scaling with the magnetic field-energy E_B. The resulting total energy emissions, E_{gw}, E_w and E_ν, produced over the lifetime of rapid spin of the black hole (12), thus become *independent* of E_B and reduce to specific fractions of E_{rot}.

When the torus is sufficiently slender, $m = 2$ modes (two lumps swirling around the black hole) develop. These radiate at essentially twice the orbital frequency of the torus, when the minor-to-major radius is less than 0.3260 by (15).

By an asymptotic analysis of (16), the gravitational-wave emissions satisfy (van Putten & Levinson 2003)

$$E_{gw} \simeq 2 \times 10^{53}\ \eta_{0.1} M_{H,7}\ E_{0.5}^{rot}\ \mathrm{erg}, \quad f_{gw} \simeq 500 \eta_{0.1} M_{H,7}^{-1}\ \mathrm{Hz}. \tag{17}$$

Thus, an "unseen" energy output (17) surpasses the true energy $E_\gamma \simeq 3 \times 10^{50}$erg in gamma-rays (Frail et al. 2001) by several orders of magnitude.

The associated output in magnetic winds contains an additional factor η, i.e.,

$$E_w \simeq 2 \times 10^{52}\ \eta_{0.1}^2 M_{H,7} E_{0.5}^{rot}\ \mathrm{erg}. \tag{18}$$

This baryon-rich wind provides a powerful agent towards collimation of any outflows from the black hole (Levinson & Eichler 2000), as well as a source of neutrinos for pick-up by the same (Levinsin & Eichler 2003). It is otherwise largely incident onto the remnant stellar envelope *from within*, which serves as energetic input to accompanying supernova ejecta. We estimate these kinetic energies to be

$$E_{SN} \simeq 1 \times 10^{51}\ \beta_{0.1} M_{H,7} \eta_{0.1}^2 E_{0.5}^{rot}\ \ \mathrm{erg} \tag{19}$$

with $\beta = v_{ej}/c$ denoting the velocity v_{ej} of supernova ejecta relative to the velocity of light c. In the expected aspherical geometry, $\beta = 0.1\beta_{0.1}$ refers to the mass-average taken over all angles. The canonical value $\beta = 0.1$ refers to the observed value in GRB011211 (Reeves et al. 2002). Eventually, the expanding remnant envelope becomes optically thin, which permits the appearance of X-ray line-emissions excited by the underlying continuum emission E_γ by dissipating E_w. The estimate (19) is in remarkable agreement with the kinetic energy 2×10^{51} erg of the aspherical supernova SN1998bw associated with GRB980425 (Höeflich et al. 1999). The energy output in MeV-neutrinos is intermediate, in being smaller than E_{gw} by an additional factor given by the slenderness parameter $\delta = qb/2R$, where b/R denotes the ratio of minor-to-major radius of the torus and q its rotation index (13). Thus, we have

$$E_\nu \simeq 1 \times 10^{53}\ \eta_{0.1} \delta_{0.30} M_{H,7} E_{0.5}^{rot}\ \mathrm{erg}, \tag{20}$$

where $\delta = 0.30\delta_{0.30}$. At the associated dissipation rate, the torus develops a temperature of a few MeV which stimulates the production of baryon-rich winds (van Putten & Levinson 2003).

6. Launching an ultrarelativistic jet by differential frame-dragging

Frame-dragging induced by angular momentum extends through the environment of the black hole and includes the spin–axis. The Kerr metric provides an exact description of this

gravitational induction process by the Riemann tensor (Chandrasekhar 1983). In turn, the Riemann tensor couples to spin (Papapetrou 1951a,b; Pirani 1956; Misner et al. 1974; Thorne et al. 1986). Specific angular momentum (angular momentum per unit mass) represents a rate of change of surface area per unit of time, while the Riemann tensor is of dimension cm^{-2} (in geometrical units). Therefore, curvature–spin coupling produces a force (dimensionless in geometrical units), whereby test particles with spin follow non-geodesic trajectories (Pirani 1956). In practical terms, the latter holds promise as a mechanism for *linear acceleration*. By dimensional analysis once more, the gravitational potential for spin–aligned interactions satisfy

$$E = \omega J \tag{21}$$

where ω denotes the local frame-dragging angular velocity produced by the black hole (or any other spinning object) and J is the angular momentum of the particle at hand. Spinning bodies therefore couple to spinning bodies (O'Connel 1972). Thus, (21) defines a mechanism for accelerating baryon-poor ejecta to ultrarelativistic velocities, provided J is large.

The angular momentum J of charged particles in strong magnetic fields, confined to individual magnetic flux-surfaces in radiative Landau states, is macroscopic in the form of orbital angular momentum

$$J = eA_{\phi}. \tag{22}$$

Here e denotes the elementary charge and $2\pi A_{\phi}$ denotes the enclosed magnetic flux, where A_a denotes the electromagnetic vector potential of an open magnetic flux-tube along the spin–axis of the black hole. Geometrically, the specific angular momentum represents the rate of change of surface area traced out by the orbital motion of the charged particle, by "helical motion" as seen in four-dimensional spacetime.

Combined, (21) and (22) describe a powerful mechanism for linear acceleration of baryon-poor matter. It radically differs from the common view, that black-hole energetic processes are limited exclusively to the action of frame-dragging in the ergosphere.

It is instructive to derive (21) by specializing to the Kerr metric on the spin–axis of the black hole. To this end, we may consider one-half the difference in potential energy of particles with angular momenta $\pm J$ suspended in a gravitational field about a rotating object. In the first case, we note that the Riemann tensor R_{ijmn} expressed relative to tetrad elements associated with Boyer-Lindquist coordinates (Chandrasekhar 1983) gives rise to a linear force

$$F_2 = JR_{3120} = -\partial_2 \omega J \tag{23}$$

which can be integrated along the spin–axis to give

$$E = \int_r^\infty F_2 ds = \omega J. \tag{24}$$

In the second case, we merely assume a metric g_{ab} with time-like and azimuthal Killing vectors and consider two particles with velocity four-vectors u^b according to angular momenta $J_\pm = g_{\phi\phi} u^t (\Omega_\pm - \omega)$,

$$J_\pm = \pm g_{\phi\phi} u^t \sqrt{\omega^2 - (g_{tt} + (u^t)^{-2}/g_{\phi\phi}} = \pm J, \tag{25}$$

which shows that u^t is the same for both particles. The total energy of the particles $E_\pm = (u^t)^{-1} + \Omega_\pm$ gives rise to

$$E = \frac{1}{2}\left(E_+ - E_-\right) = \omega J. \tag{26}$$

To apply (21-22) to gamma-ray bursts from rotating black holes, consider a perfectly conducting blob of charged particles in a magnetic flux-tube subtended at a finite half-opening angle θ_H on the event horizon of the black hole and along its spin–axis. In the approximation of electrostatic equilibrium, it assumes a rigid rotation (Thorne et al. 1986) described by an angular velocity Ω_b. (By Faraday induction, differential rotation introduce potential differences along magnetic field-lines. Some differential rotation is inevitable over long length scales and, possibly, in the formation of gaps). In the frame of zero-angular momentum observers, the equilibrium charge-density assumes the value of Goldreich & Julian (1969), as viewed by zero-angular momentum observers. Thus, given a number $N(s)$ of charged particles per unit scale height s in the flux-tube,

$$N(s) = (\Omega_b - \omega) A_\phi / e. \tag{27}$$

A pair of blobs of scale height $h = h_M M_H$ in both directions along the spin–axis of the black hole each hereby receive a potential energy

$$E_b = \omega J N h = 10^{47} B_{15} h_M^3 H \text{ erg}, \tag{28}$$

where $B = B_{15} \times 10^{15}$G and $H = 4\hat{\omega}\left(\hat{\Omega}_b - \hat{\omega}\right)$ is a quantity of order unity, expressed in terms of the normalised angular velocities $\hat{\omega} = \omega/\Omega_H$ and $\hat{\Omega}_b = \Omega_b/\Omega_H$.

Electrons and positrons in superstrong magnetic fields are essentially massless. The ejection of a pair of blobs with energy (28) thus takes place in a light-crossing time of about 0.3ms of, e.g., seven solar mass black hole of linear dimension 10^7cm. This corresponds to

in an instantaneous luminosity of about 3×10^{50}erg/s. This produces a total kinetic energy output of up to 10^{52} erg in tens of seconds in long bursts. A fraction hereof which will be dissipated in gamma-rays and lower-energy afterglow emissions in the internal-external shock model for GRBs (Rees & Mészáros 1992, 1994).

Similar results obtain by considering the luminosity in a steady-state limit, by considering a horizon half-opening angle $\theta_H \simeq M_H/R$, set by the poloidal curvature M_H/R of the magnetic field-lines. We note the paradoxical *small* energy output of GRB-afterglow emissions, when viewed relative to the total black-hole spin–energy (2). The luminosity in the jet scales with the square of the enclosed magnetic flux, while the latter scales with the enclosed surface area, and hence the square of the half-opening angle θ_H. Thus, we encounter a geometrical scale-factor, which creates a jet luminosity

$$L_j \propto \theta_H^4. \tag{29}$$

Even when θ_H is not small, e.g., about 10 degrees, this scaling creates a small parameter. Integrated over time, the energy output in gamma-rays satisfies (van Putten & Levinson 2003)

$$E_\gamma \simeq 1 \times 10^{50} \epsilon_{0.3} \eta_{0.1}^{8/3}\ E_{0.5}^{rot}\ \text{erg}, \tag{30}$$

consistent with the observed true energy output 3×10^{50} erg in gamma-rays of long bursts (Frail et al. 2001), where $\eta = 0.1\eta_{0.1}$ and $\epsilon = 0.3\epsilon_{0.3}$ denotes the efficiency of converting kinetic energy to gamma-rays.

In our unification scheme, the durations of short and long bursts are attributed to different spin-down times of, respectively, a slowly and rapidly spinning black hole according to (12). The total energy output in gamma-rays of short GRBs is hereby significantly smaller than that of long GRBs, due to both shorter durations and smaller luminosities. In this light, the recent X-ray afterglow detections to short bursts, very similar but fainter than their counterparts to long bursts, are encouraging.

7. Long-duration bursts in gravitational-waves

The output in gravitational radiation (17) is in the range of sensitivity of the broad band detectors LIGO and Virgo shown in Fig. 5, as well as GEO (Danzmann 1995; Willke et al. 2002) and TAMA (Ando et al. 2002). Note that the match is better for higher-mass black holes, in view of their emissions at lower frequencies (towards the minimum in the detector noise curve) and their larger energy output.

Matched filtering gives a theoretical upper bound on the signal-to-noise ratio in the detection of long bursts in gravitational radiation from GRB-supernovae. In practice, the frequency will be unsteady at least on an intermittent timescale associated with the evolution of the torus, e.g., due to mass-loss in winds and possibly mass-gain by accretion from additional matter falling in. For this reason, a Time-Frequency Trajectory method which correlates the coefficients of a Fourier transformation over subsequent windows of durations of seconds might apply. The ultimate signal-to-noise ratio will therefore be intermediate between that obtained through correlation – a second-order procedure – and matched filtering – a first-order procedure. The results shown in Fig. 5 show the maximal attainable signal-to-noise ratio (by matched filtering) for sources at a fiducial distance of 100Mpc. This distance corresponds to an event rate of one per year.

GRB-supernovae are an astrophysical source population locked to the star-formation rate. We can calculate their contribution to the stochastic background in gravitational radiation accordingly given their band-limited signals, assuming $B = \Delta f/f_e$ of around 10%, where f_e denotes the average gravitational-wave frequency in the comoving frame. In what follows, we the following scaling relations are applied,

$$E_{gw} = E_0 M_H/M_0, \quad f_e = f_0 M_0/M_H \tag{31}$$

where $M_0 = 7M_\odot$, $E_0 = 0.203 M_\odot \eta_{0.1}$ and $f_0 = 455\mathrm{Hz}\eta_{0.1}$, assuming maximal spin–rates ($E_{rot} = E_{rot,max}$). For non-extremal black holes, a commensurate reduction factor in energy output can be inserted. This factor carries through proportionally to the final results, whence it is not taken into account explicitly.

Summation over a uniform distribution of black hole masses, e.g., $M_H = (4--14)\times M_\odot$, and assuming that the black hole mass and η in (6), are uncorrelated, the expected spectral energy-density satisfies (van Putten et al. 2004)

$$< \epsilon'_B(f) >= 1.08 \times 10^{-18} \hat{f}_B(x) \text{ erg cm}^{-3} \text{ Hz}^{-1} \tag{32}$$

where $\hat{f}_B(x) = f_B(x)/\max f_B(\cdot)$ is a normalized frequency distribution. The associated dimensionless amplitude $\sqrt{S_B(f)} = \sqrt{2G/\pi c^3} f^{-1} \tilde{F}_B^{1/2}(f)$, where $\tilde{F}_B = c\epsilon'_B$ and G denotes Newton's constant satisfies

$$\sqrt{S_B(f)} = 7.41 \times 10^{-26} \eta_{0.1}^{-1} \hat{f}_S^{1/2}(x) \text{ Hz}^{-1/2} \tag{33}$$

where $\hat{f}_S(x) = f_S(x)/\max f_S(\cdot)$, $f_S(x) = f_B(x)/x^2$, Likewise, we have for the spectral closure density $\Omega_B(f) = f\tilde{F}_B(f)/\rho_c c^3$ relative to the closure density $\rho_c = 3H_0^2/8\pi G$

$$\tilde{\Omega}_B(f) = 1.60 \times 10^{-8} \eta_{0.1} \hat{f}_\Omega(x), \tag{34}$$

where $\hat{f}_\Omega(x) = f_\Omega(x)/\max f_\Omega(\cdot)$, $f_\Omega(x) = x f_B(x)$ and H_0 denotes the Hubble constant.

These cosmological results show a simple scaling relation for the extremal value of the spectral closure density in its dependency on the model parameter η. The location of the maximum scales with f_0 in view of $x = f/f_0$. The spectral closure density thus becomes completely determined by the shape of the function representing the star-formation rate, the fractional GRB-supernova rate thereof, η, and the black-hole mass distribution. Fig. 5 shows the various distributions. The extremal value of $\Omega_B(f)$ is in the neighborhood of the location of maximal sensitivity of LIGO and Virgo. It would be of interest to search for this contribution to the stochastic background in gravitational waves by correlation in the spectral domain, following Fourier transformation over series of sub-windows on intermediate timescales of seconds.

8. Conclusions

The sixties saw two independent discoveries: the first GRB670702 by the Vela satellite and the exact solution of rotating black holes by Roy P. Kerr. Through observational campaigns with BATSE, BeppoSax, the Interplanetary Network (IPN), HETE-II and now Swift, we have come to understand the phenomenology of GRBs. Long bursts are association with supernovae, representing a rare and extraordinary powerful cosmological transient, taking place about once a minute and reaching the earliest epochs in the Universe. Independently, through the works of Penrose (1969); Ruffini & Wilson (1975); Blandford & Znajek (1977) and others, we have come to understand the potential significance of Kerr black holes as compact, baryon-free energy sources with certain universal properties. The applications to high-energy astrophysics should be enormous (e.g. Levinson (2004)), of supermassive black holes in active galactic nuclei including our own galaxy (Porquet et al. 2004), and of stellar mass black holes in microquasars (Mirabel & Rodrǵuez 1994) and, possibly, gamma-ray bursts.

While the formation-process of supermassive black holes remains inconclusive, the birthplace of stellar mass black holes is most probably core-collapse supernovae of massive stars. Evidence for Kerr black holes as the energy source to high-energy astrophysical processes remains elusive, however. Recent measurements on frame-dragging by X-ray spectroscopy, typically during inactive states of the black hole, are encouraging in this respect (A.C. Fabian, these proceedings).

Specically, we propose that GRB-supernovae are powered by rapidly rotating black holes, wherein (1) the durations of long GRBs of tens of seconds are identified with the

lifetime of rapid spin of the black hole in a state of suspended accretion, (2) an accompanying supernova is radiation-driven by magnetic winds from a torus in suspended accretion, (3) ultrarelativistic outflows are launched by gravitational spin-orbit coupling with charged particles along open magnetic field-lines, and (4) a small branching ratio of Type Ib/c supernovae into GRBs is attributed to the small probability of producing black holes with small kick velocities.

Modeling short GRBs from slowly rotating black holes, we predicted X-ray afterglows very similar but weaker (in total energies) than those of long bursts. The recent discovery of faint X-ray afterglows to GRB050509B and GRB050709 fit well within this scheme.

Gamma-ray bursts present a potentially powerful link between rotating black holes and gravitational radiation. Strategic searches for their chirps in binary coalescence of neutron stars and black holes, or long-duration bursts in gravitational radiation during radiative spin-down of a high-mass black hole, can be pursued by the advanced detectors LIGO and Virgo. Strategic searches are preferrably pursued in combination with upcoming optical-radio supernova surveys, e.g., Pan-Starrs in Hawaii (Kudritzki 2003) in combination with the Low Frequency Array (LOFAR 2005), see also Gal-Yam (2005). In light of the proposed supernova-like signatures from the debris of a neutron star (Kulkarni 2005), these strategies might apply to both short and long bursts.

LIGO and Virgo promise to bring together a serendipitous discovery and general relativity, providing a unique method to identify Kerr black holes as the most luminous objects in the Universe.

Acknowledgment. The author thanks A. Levinson, R.P. Kerr, R. Preece, and David Wiltshire for constructive comments. This research is supported by the LIGO Observatories, constructed by Caltech and MIT with funding from NSF under cooperative agreement PHY 9210038. The LIGO Laboratory operates under cooperative agreement PHY-0107417. This paper has been assigned LIGO document number LIGO-P040013-00-R.

REFERENCES

Abramovici, A., Althouse, W.E., Drever, R.W.P., et al., 1992, Science, 292, 325

Acernese, F., et al., 2002, Class. Quant. Grav., 19, 1421

Akiyama, S., Wheeler, J.C., Meier, D.L., Lichtenstadt, I., 2003, ApJ, 584, 954

Ando, M., and the TAMA Collaboration, 2002, Class. Quant. Grav., 19, 1409

Bardeen, J.M., 1970, Nature, 226, 64

Bardeen, J.M., Press, W.H., & Teukolsky, S.A., 1972, ApJ, 178, 347

Barish, B., & Weiss, R., 1999, Phys. Today, 52, 44

Bekenstein, J.D., 1973, ApJ, 183, 657

Bethe, H.A., Brown, G.E., & Lee, C.-H., 2003, Selected Papers: Formation and Evolution of Black Holes in the Galaxy (World Scientific), p262

Bisnovatyi-Kogan, G.S., 1970, Astron. Zh., 47, 813

Bisnovatyi-Kogan, G.S., Popov, Yu. P., & Samochin, A.A., 1976, Ap & S.S., 41, 287

Blandford, R. D., and Znajek, R. L. 1977, MNRAS, 179, 433

Bonnell, I.A. & Pringle, J.E., 1995, MNRAS, 273, L12

Bradaschia, C., Del Fabbro, R., di Virgilio, A., et al., 1992, Phys. Lett. A, 163, 15

Bromberg, O., Levinson, A., & van Putten, M.H.P.M., 2005, astro-ph/0507078

Brown, G.E., Lee, C.-H., Wijers R.A.M.J., Lee, H.K., Israelian G. & Bethe H.A., 2000, NewA, 5, 191

Burrows, A., & Lattimer, J.M., 1987, ApJ, 318, L63

Chandrasekhar, S., 1983, The Mathematical Theory of Black Holes, Oxford University Press, Oxford

Chincarini, G., et al., 2005, ApJ, submitted

Costa, E., et al., 1997, Nature, 387, 878

Davies, M.B., King, A., Rosswog, S., & Wynn G., 2002, ApJ, 579, L63

Danzmann, K., 1995, in First Edoardo Amaldi Conf. Grav. Wave Experiments, E. Coccia, G. Pizella, F. Ronga (Eds.), World Scientific, Singapore, p100

Duez, M.D., Shapiro, S.L., & Yo, H.-J., 2004, Phys. Rev. D., 69, 104016

Faber, J.A., Grandclément, P., & Rasio, F., 2004, Phys. Rev. D., 124036

Filipenko, A.V., 1997, ARA&A, 35, 309

Finn, L.S., Krishnan, B., & Sutton, P.J., 2004, ApJ, 607, 384

Fox, D.B., et al., 2005, Nature, 437, 845

Frail, D.A., et al., 1997, Nature, 389, 261

Frail, D.A., Kulkarni, S.R., Sari, R., et al., 2001, ApJ, 562, L55

Fryer, C.L., Woosley, S.E., Herant, M., & Davies, M.B., 1999, ApJ, 520, 650

Fryer, C.L., Holz, D.E., & Hughes, S.A., 2002, ApJ, 565, 430

McFadyen, A.I. & Woosley, S.E., 1999, 524, 262

Gal-Yam, A., et al., 2005, ApJ, submitted; astro-ph/0508629

Gehrels, N., et al., 2005, Nature, 437, 851

Goldreich, P., & Julian, W.H., 1969, ApJ, 157, 869

Goldreich, P., Goodman, J., & Narayan, R., 1986, MNRAS, 221, 339

Haislip, J.B., et al., 2005, Nature, submitted

Hawking S.W., 1975, Commun. Math. Phys., 43:199

Heise, J., in 't Zand, J., Kippen, R.M., & Woods, P.M., in Gamma-ray Bursts in the Afterglow Era, CNR, 2000, ed. E. Costa, F. Frontera & J. Hjorth, Berlin: Springer 2001, p16

Hjörth, J., et al., 2005, Nature, 437, 859

Höflich, P.J., Wheeler, J.C., Wang, L., 1999, ApJ, 521, 179

Hulse, R.A., & Taylor, J.H., 1975, ApJ, 195, L51

Katz, J.I., 1994, 432, L27

Keller, H.B., 1987, Numerical Methods in Bifurcation Problems (Berlin: Springer/Tata Inst. Fundam. Res.)

Kerr, R.P., 1963, Phys. Rev. Lett., 11, 237

Klebesadel, R., Strong I. and Olson R., 1973, ApJ, 182, L85

Kobayashi, S., Mészáros, P., 2003, ApJ, 582, L89

Kobayashi, S., Mészáros, P., 2003, ApJ, 582, L89

Kouveliotou, C., Meegan, C.A., Fishman, G.J., et al., 1993, ApJ, 413, L101

Kudritzki, R., 2003, private commun. (see http://www.ifa.hawaii.edu/pan-starrs)

Kulkarni, S.R., 2005, astro-ph/0510256

Kundt, W., 1976, Nature, 261, 673

Landau, L.D., & Lifschitz, E.M., 1984, Classical Theory of Fields, Pergamon Press, Oxford

LOFAR (see http://www.lofar.org)

LeBlanc, J.M., & Wilson, J.R., 1970, ApJ, 161, 541

Lee, C.-H., Brown, G.E., & Wijers, R.A.M.J., 2002, ApJ, 575, 996

Levinson A., van Putten, M.H.P.M., 1997, ApJ, 488, 69

Levinson, A., & Eichler, D., 2000, Phys. Rev. Lett., 85, 236

Levinson, A., & Eichler, D., 2003, ApJ, 594, L19

Levinson, A., 2004, ApJ, 608, 411

Maund, J.R., Smartt, S.J., Kudritzki, R.P., Podsiadiowski, P., & Gilmore,, G.F., 2004, Nature, 427, 129

Mazets, E.P., Golenetskii, S.V. and Ilinskii, V.N., 1974, JETP, 19, L77

Meegan, C.A., Fishman, G.J., Wilson, R.B., et al., 1992, Nature, 355, 143

Mészáros, P., & Rees, M.J., 1993, ApJ, 405, 278

Mineshige, S., Takashi, H., Mami, M., & Matsumoto, R., 2002, PASJ, 54, 655

Mirabel, I.F. & Rodríguez, L.F. 1994, Nature, 371, 46

Misner, C.W., Thorne, K.S., Wheeler, A., 1974, Gravitation (San Francisco)

Nakamura, T., & Fukugita, M., 1989, ApJ, 337, 466

Nomoto, K., Iwamoto, K., & Suzuki, T, 1995, Phys. Rep. 256, 173

O'Connel, R.F., 1972, Phys. Rev. D., 10, 3035

Okamoto, I., 1992, MNRAS, 253, 192

Paciesas, W.S. 1999, ApJ Suppl, 122, 465

Paczyński, B.P., 1991, Acta. Astron., 41, 257

Paczyński, B.P., 1998, ApJ, 494, L45

Papadopoulos, P., & Font, J.A., 2001, Phys. Rev. D., 63, 044016

Papaloizou, J.C.B., & Pringle, J.E., 1984, MNRAS, 208, 721

Papapetrou, A., 1951, Proc. Roy. Soc., 209, 248

Papapetrou, A., 1951, Proc. Roy. Soc. 209, 259

Penrose, R., 1969, Rev. del Nuovo Cimento, 1, 252

Peters, P.C., and Mathews, J., 1963, Phys. Rev., 131, 435

Pirani, F.A.E., 1956, Act. Phys. Pol., XV, 389

Piran, T., 2004, Rev. Modern Phys., to appear; astro-ph/0405503

Piro, L., 2005, Nature, 437, 822

Porquet, D., et al., 2004, A&A, 407, L17

Press W.H. and Teukolsky S.A., 1972, ApJ., 178, 347

Rampp, M., Müller, E., & Ruffert, M., 1998, A&A, 332, 969

Rees, M.J., Ruffini, R., & Wheeler, J.A., 1974, *Black Holes, Gravitational Waves and Cosmology: an introduction to current research* (Gordon & Breach, New York), Section 7

Rees, M.J., & Mészáros, P., 1992, MNRAS, 258, 41P

Rees, M.J., & Mészáros, P., 1994, ApJ, 430, L93

Reeves, J.N., Watson, D., Osborne, J.P., 2002, Nature, 416, 512

Ruffini, R., & Wilson, J.R., 1975, Phys. Rev. D., 12, 2959

Spallici, A.D.A.M., Aoudia, S., de Freitas Pacheco, J.A., et al. 2004, gr-qc/0406076

Stanek, K.Z., Matheson, T., Garnavich, P.M., et al., 2003, ApJ, 591, L17

Starobinsky, A.A., 1972, Zh. ETF, 64, 48 [Sov. Phys. JETP,37:28 (1973)]

Taylor, J.H., 1994, Rev. Mod. Phys., 66, 711

Teukolsky S.A., 1973, ApJ., 185, 635

Teukolsky, S.A., &, Press, W.H., 1974, ApJ., 193, 443

Thorne, K.S., Price, R.H., MacDonald, D.A., 1986, Black Holes: The Membrane Paradigm, Yale University Press, New Haven, CT

Turatto, M., 2003, in Supernovae and Gamma-ray Bursters, ed. K.W. Weiler (Springer-Verlag, Heidelberg), p21

Unruh W.G., 1974, Phys. Rev. D., 10, 3194

Villasenor, J.S., et al., 2005, Nature, 437, 855

van Paradijs, J., et al., 1997, Nature, 386, 686

van Putten, M.H.P.M., & Ostriker, E.C., 2001, ApJ, 552, L31

van Putten, M.H.P.M., 2002, ApJ, 575, L71

van Putten, M.H.P.M., & Levinson, A., 2003, ApJ, 584, 953

van Putten, M.H.M.P., & Regimbau, T., 2003, ApJ, 593, L15

van Putten, M.H.P.M., 2004, ApJ, 611, L81

van Putten, M.H.P.M., Levinson, A., Lee, H.-K., Regimbau, T., & Harry, G., 2004, Phys. Rev. D., 69, 044007

Wheeler, J.C., Yi, I., Höflich, P., Wang, L., 2000, ApJ, 537, 810

Willke, B., et al., 2002, Class. Quant. Grav., 19, 1377

Woosley, S.E., 1993, ApJ, 405, 273

Zel'dovich Ya. B., 1971, Zh. Eks. Teor. Fiz., 14, 270 [transl. JETP Lett. 14,180(1971)]

Zhuge, X., Centrella, J.M., McMillam, S.L.W., Phys. Rev. D., 50, 6247

Table Captions

Table I. Trigonometric parametrization of a Kerr black hole. Here, M denotes the mass of the black hole, $a = J_H/M$ denotes the specific angular momentum, E_{rot} the rotational energy and M_{irr} denotes the irreducible mass.

Figure Captions

Fig. 1 (*Left*) A histogram of redshift-corrected distributions of 27 long bursts with individually determined redshifts from their afterglow emissions. It shows durations $T_{90}/(1+z)$ of tens of seconds at a mean redshift distance $< z >= 1.25$, indicative of their cosmological distances. (*Right*) The optical spectrum of the Type Ic SN2003dh associated with GRB030329 is remarkably similar to that of the Type Ic SN1998bw of GRB980425 one week before maximum. GRB030329 displayed a gamma-ray luminosity of about 10^{-1} times typical at a distance of $z = 0.167$ ($D \simeq 800$Mpc), whereas GRB980425 was observed at anomalously low gamma-ray luminosity (10^{-4} times typical) in the local universe ($z = 0.008, D \simeq 37$Mpc). At the same time, their supernovae were very luminous with inferred ^{56}Ni ejecta of about $0.5M_{\odot}$. (Reprinted from van Putten (2002); Stanek et al. (2003)©The American Astronomical Society.)

Fig. 2 (*Left*) Black holes with small kick velocities remain centered in core-collapse of a uniformly rotating massive star. Shown is the accumulated specific angular momentum of the central object (arbitrary units) versus dimensionless orbital period $1/\beta$. Arrows indicate the evolution as a function of time. Kerr black holes exist *inside* the outer curve (diamonds). A black hole forms in a first-order transition following the formation and collapse of a torus. This produces a short burst in gravitational radiation. When centered, the black hole surges to a high-mass object by direct infall of matter with relatively low specific angular momentum, up to the inner continuous curve (ISCO). At this point, the black hole either spins up by continuing accretion or spins down radiatively against gravitational radiation emitted by a surrounding non-axisymmetric torus. In this state, the black hole creates a baryon poor jet as input to GRB-afterglow emissions. This continues until the angular velocity of the black hole equals that of the torus (dot-dashed line). This scenario fails for black holes with typical kick velocities with inevitable escape from the high-density core, prohibiting the formation of a high mass black hole surrounded by a high-mass torus. The probability of small kick velocities defines the branching ratio of Type Ib/c supernovae into long GRBs. (*Right*) The black hole mass M and rotational energy E_{rot} of formed after surge in case of small kick velocities, expressed relative to the mass M_{He} of the progenitor He-star. The results are shown in cylindrical geometry (continuous) and spherical geometric (dashed). Note the broad distribution of high-mass black holes with large rotational energies

of $5-10\%$ (spherical to cylindrical) of $M_{He}c^2$. (Reprinted from van Putten (2004)©The American Astronomical Society.)

Fig. 3 A uniformly magnetized torus represented by two counter-oriented current rings around a black hole (C) forms out of both core-collapse (A1-B1) in massive stars and tidal break-up (A2-B2) in black hole-neutron star coalescence, followed by a single reconnection event (B2-C). (Reprinted from van Putten & Levinson (2003)©The American Astronomical Society.)

Fig. 4 The stability diagram showing the neutral stability curves for non-axisymmetric buckling modes in a torus of an inviscid incompressible fluid of arbitrary minor-to-major radius b/a. Curves of critical rotation index q_c are labeled with azimuthal quantum number $m = 1, 2, \cdots$, where instability sets in above and stability sets in below. (Reprinted from van Putten (2002)©The American Astrophysical Society.)

Fig. 5 (*Left*) GRB-supernovae from rotating black holes predict a contemporaneous long-duration burst in gravitational radiation within the range of sensitivity of upcoming gravitational-wave detectors LIGO and Virgo within a distance of about 100Mpc. The corresponding event rate is about one per year. The "blue bar" denotes the distribution of dimensionless strain amplitudes for a distribution of sources corresponding to a range of black hole masses and efficiency factors, assuming matched filtering. In practice, the sensitivity will depend less on using time frequency trajectory methods with correlations in the spectral domain. (*Right*) The cosmological distribution of GRB-supernovae is locked to the star-formation rate $N(z)$. This enables the calculation of the expected contribution to the stochastic background in gravitational radiation, here shown in terms of the spectral energy-density $\epsilon'_B(f)$, the strain amplitude $S_B^{1/2}(f)$ and the spectral closure density $\Omega_B(f)$. The results are calculated for uniform mass-distributions of the black hole, $M_H = (4-14) \times M_\odot$ (top curves) and $M_H = (5-8) \times M_\odot$ (lower curves) with $\eta = 0.1$ (solid curves) and $\eta = 0.2$ (dashed curves). The extremal value of $\Omega_B(f)$ is in the neighborhood of maximal sensitivity of LIGO and Virgo. (Reprinted from van Putten et al. (2004)©2004 American Physical Society.)

Table 1:

Symbol	Expression	Comment
λ	$\sin\lambda = a/M$	
Ω_H	$\tan(\lambda/2)/2M$	
J_H	$M^2 \sin\lambda$	
E_{rot}	$2M \sin^2(\lambda/4)$	$\leq 0.29M$
M_{irr}	$M \cos(\lambda/2)$	$\geq 0.71M$

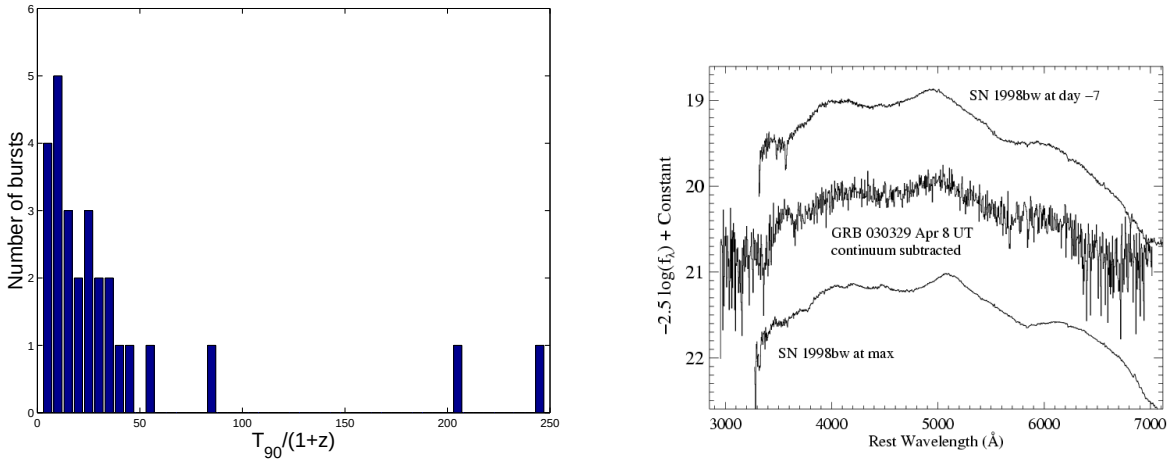

Fig. 1.—

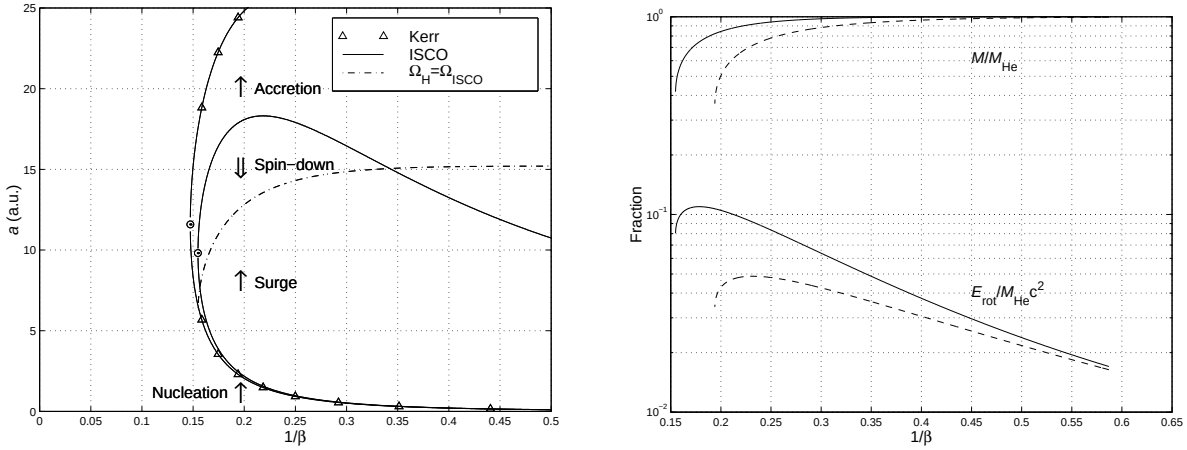

Fig. 2.—

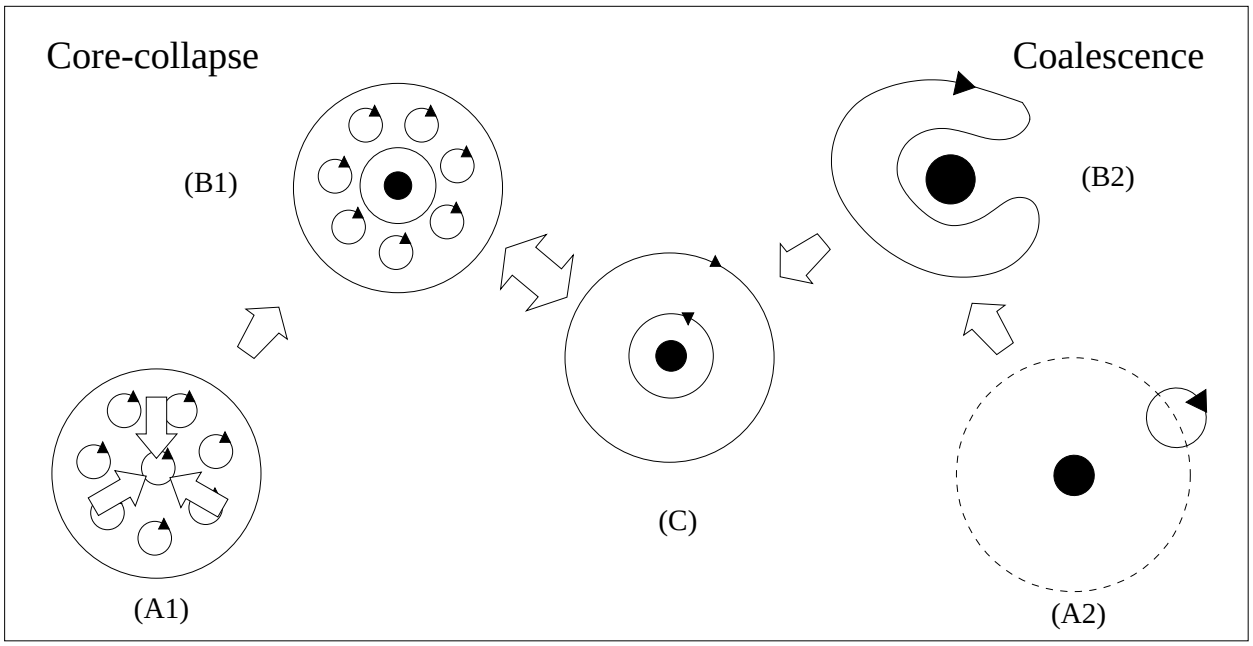

Fig. 3.—

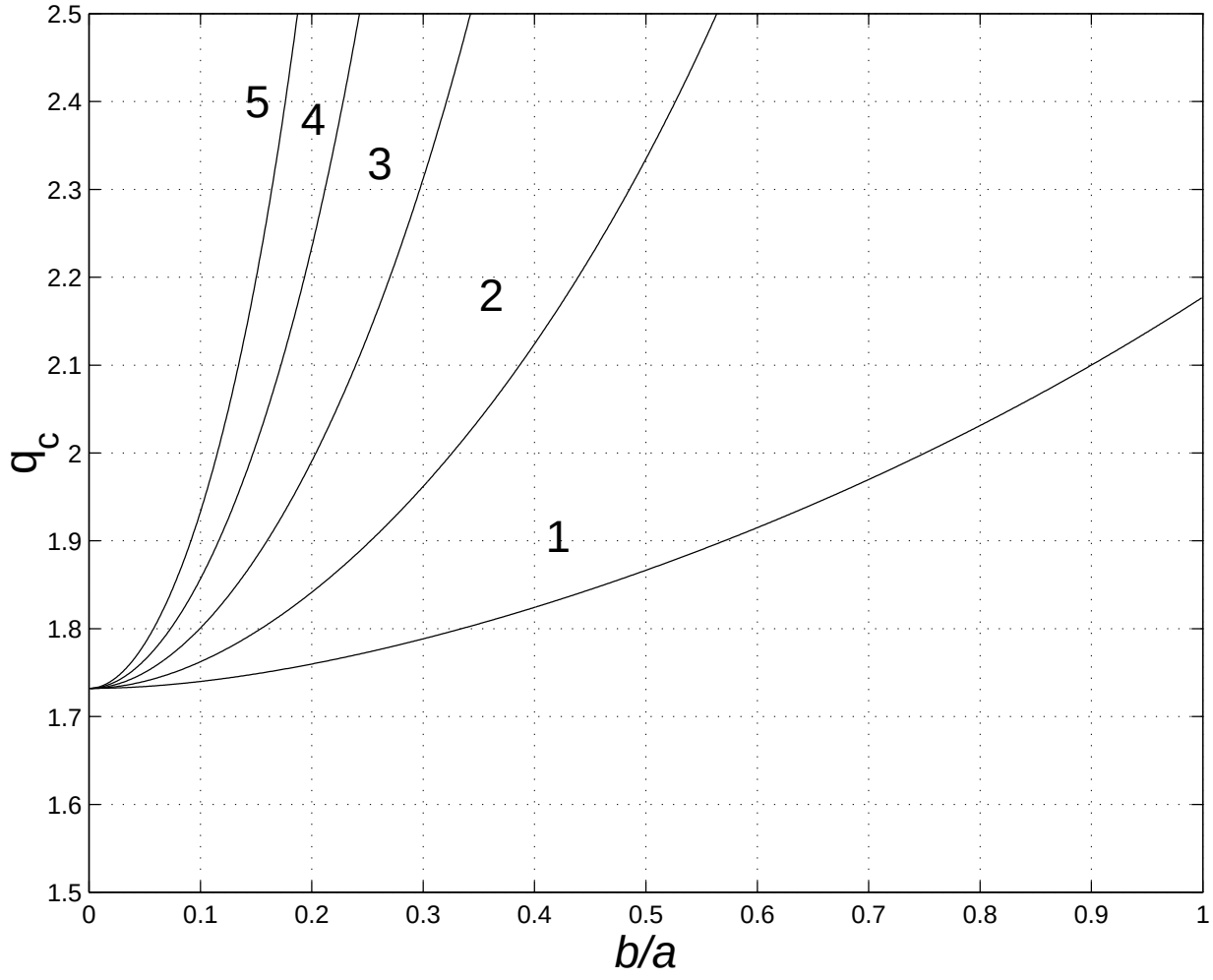
2.5
2.4
2.3
2.2
2.1
2
1.9
1.8
1.7
1.6
1.5
q_c
0
0.1
0.2
0.3
0.4
0.5
0.6
0.7
0.8
0.9
1
b/a
5
4
3
2
1

Fig. 4.—

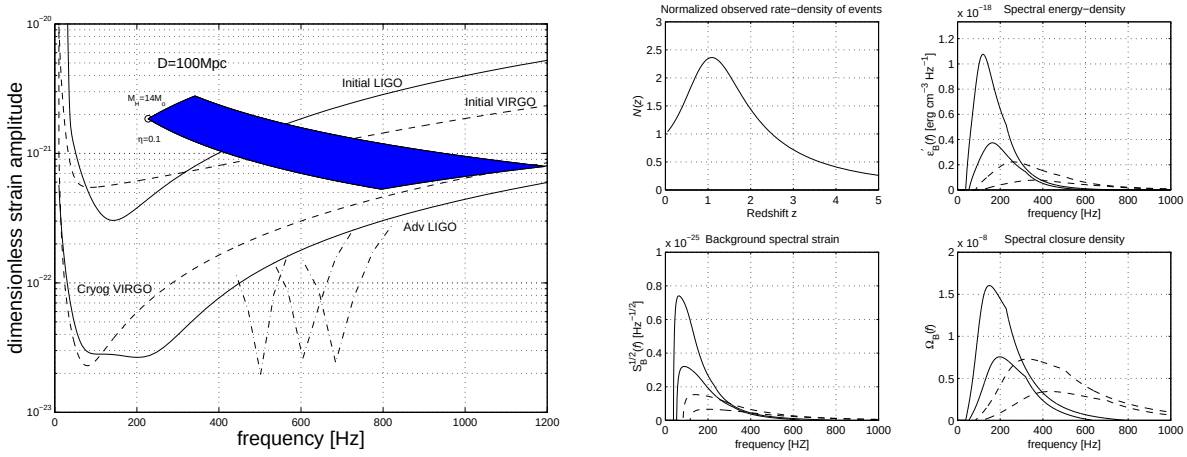
D=100Mpc
Initial LIGO
Initial VIRGO
Adv LIGO
Cryog VIRGO
dimensionless strain amplitude
frequency [Hz]
Normalized observed rate−density of events
N(z)
Redshift z
Spectral energy−density
frequency [Hz]
Background spectral strain
frequency [HZ]
Spectral closure density
frequency [Hz]

Fig. 5.—